Chapter 7
Thixocasting

Abstract Following a very detailed analysis of rheocasting, this chapter concentrates on thixocasting as another alternative route for SSM processing of metallic alloys. The effect of reheating parameters on the resulted microstructure of SSM billets is studied in detail and the effect of grain refining on the final structure of thixocast alloys is highlighted. The issue of liquid entrapment is discussed with respect to grain refinement.

7.1 Introduction

The previous chapters have dealt with the process of SSM casting directly from the melt, that is, rheocasting. The slurry is prepared by stirring the superheated molten alloy as it cools down to the mushy zone. This chapter describes thixocasting process where reheating of the alloy to temperatures above solidus and holding it isothermally within the mushy zone induces the desired structure for SSM casting.

One of the important issues in deciding whether to switch to one specific SSM fabrication route is the supply of feedstock. The term Slurry on Demand (SoD) describes the slurry-making operations to provide a constant supply of slurry for shaping operations. This may include the billets (slugs) produced via conventional casting or rheocasting, stored and used later by simple and short reheating to mushy zone. This in fact prescribes the SoD procedure based on a combination of rheocasting and thixocasting. Such an approach could be beneficial to establish manufacturing plants in regions with restricted environmental regulations while the feedstock can be produced in specialized sites and shipped to the manufacturing plants to fulfill the SoD requirements. This is similar to mini mills for steel industry where the feed stock is shipped to mills to be reheated and rolled to plates and sheets. Therefore, it is necessary to discuss the process of thixocasting to provide a basis for comparison.

S. Nafisi, R. Ghomashchi, *Semi-Solid Processing of Aluminum Alloys*,
DOI 10.1007/978-3-319-40335-9_7

7.2 Thixocasting of the Refined Conventional Cast Specimens

Limited series of tests were performed by reheating the specimens prepared for thermal analysis (Sect. 4.1). The main objective was to verify the effectiveness of inoculation during the reheating stage. Samples were chosen according to the results obtained in Sect. 6.2.1. During the entire experiments, three critical parameters were investigated: effect of partial remelting time, solidification cooling rate, and type of the refiner. These include 5 and 10 min reheating time, two different cooling rates during solidification process, and addition of sole B and Ti−B via Al5B and Al5Ti1B master alloys, respectively.

7.2.1 Effect of Reheating Time on SSM Structure

Figure 7.1 shows microstructural evolution of as-cast solidified samples in graphite cup which partially remelted at 583 ± 3 °C (Sect. 4.1.1.4). At this temperature, there is about 38–40 % fraction solid according to ThermoCalc calculations. During partial remelting and subsequent isothermal holding, there are several mechanisms active as follows:

- Remelting of low melting points constituents, eutectic mixture
  At this stage, the α-Al portion of the eutectic phase gradually precipitates on the α-Al primary phase leading to their growth. Numerous examples will be provided in this chapter (it is important to consider that the majority of eutectic phase is α-Al).
- Grain coarsening and ripening
  Dendrite fragmentation and coalescence could happen at the same time. Roots of some dendrite arms may get narrow, detach, and form separate particles. Also coalescence may result in liquid entrapment.
- Globularization and further particle coarsening
  Diffusion from areas with higher radius of curvature to areas with lower radius of curvature to decrease the interfacial energy between solid–liquid.

As shown in Fig. 7.1a, the as-cast untreated structure has a dendritic morphology. Other than coarsening of dendrites, reheating for 5 min seems had no major structural variation. After 10 min isothermal holding, the initial dendritic structure becomes thicker and rounder but still far from globular structure. In fact, the final microstructure is highly dependent on the original as-cast structure. Nevertheless, at the initial stage of holding, the main development is remelting of the eutectic regions which were indeed the last region to form during solidification process. For dendritic solidification, the eutectic already formed between the secondary or tertiary arms which by reheating process, this liquid is more likely to be entrapped within the arms. Meanwhile other mechanisms are in operation as well.

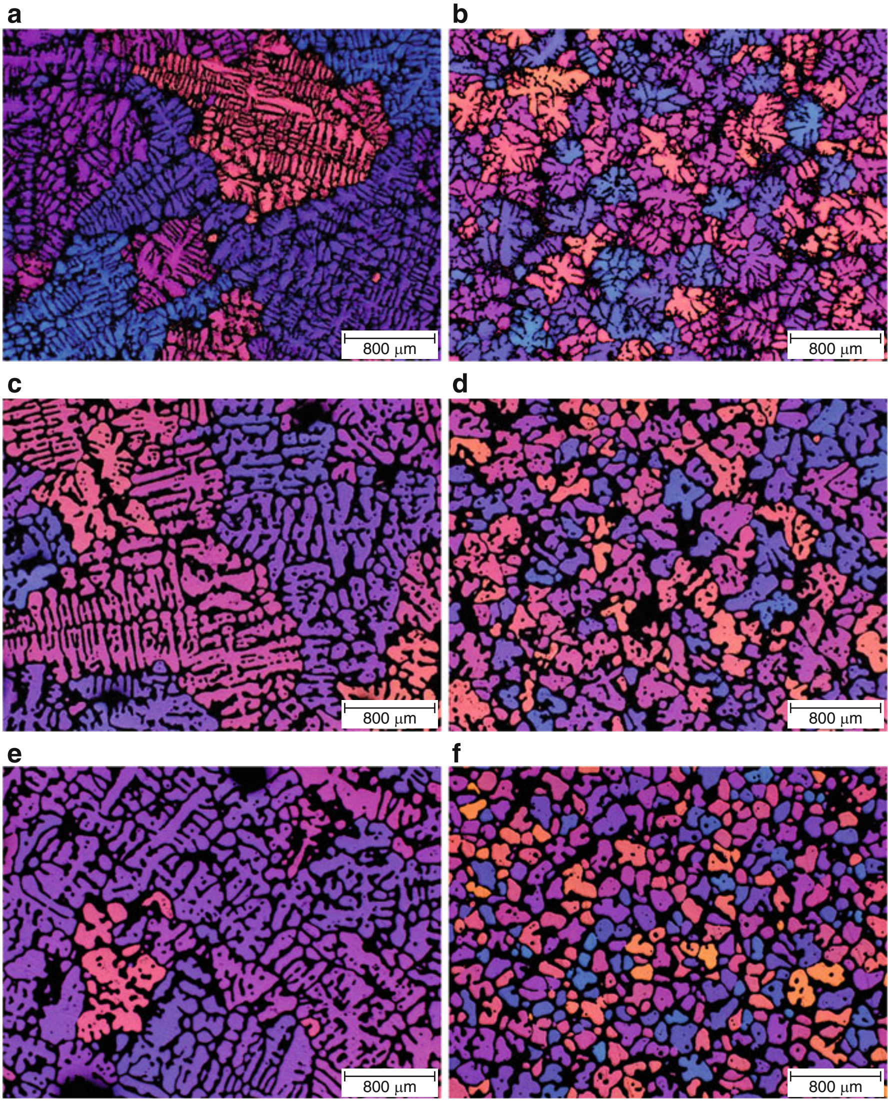

Fig. 7.1 Polarized light micrographs; (**a**), (**c**), (**e**) A356, untreated, (**b**), (**d**), (**f**) A356 with 226 ppm B (as-cast "(**a**), (**b**)", 5 min "(**c**), (**d**)", and 10 min "(**e**), (**f**)" reheated samples and isothermally held at 583 °C)

Grain coarsening leads to thicker secondary arms. By ripening, the smaller grains remelt and the larger ones grow. Ripening of secondary dendrite arms is quite evident which is due to the reheating time/temperature and tendency of the structure to reach the lower energy level, specifically rounder particles.

In Sect. 6.2, various refiners were used to evaluate their effectiveness and it was found that the addition of sole boron results in minimum average grain size.

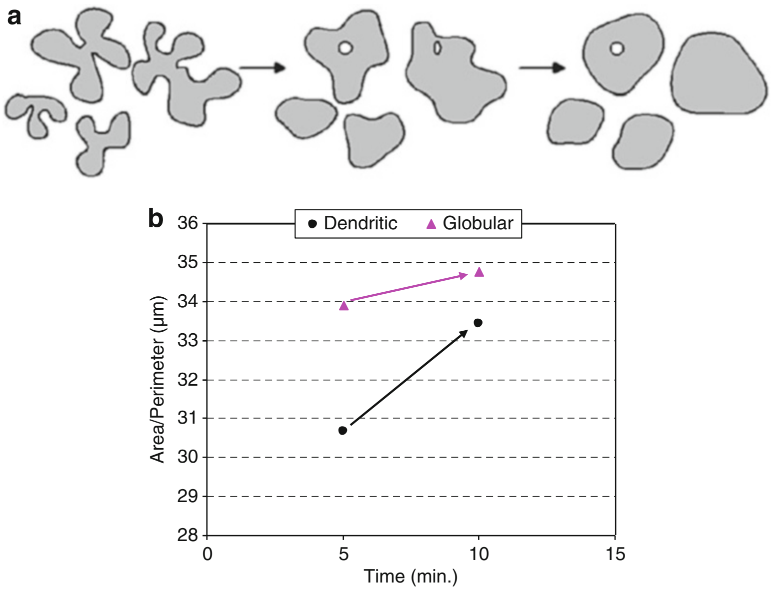

Fig. 7.2 (**a**) Schematic presentation of evolution toward globules formation, (**b**) solid–liquid interfacial evolution as a function of holding time (*circles* for untreated A356 and *triangles* for A356 refined with boron)

Consequently, boron was found as an excellent refiner to alter the dendritic structure even with high superheat casting process. After 5 min isothermal heating at 583 °C, the structure had lost the initial dendritic structure and evolved into more chunky and isolated particles resembling rosette/globule morphology. By 10 min reheating, the structure becomes almost globular with nearly uniform particle size. The liquid entrapped within the α-Al particles is reduced in timely manner and most of it well distributed between α-Al particles (Fig. 7.1).

The driving force for the evolution toward globularization is the reduction of the eutectic-primary particles interface area. This could be interpreted in terms of A/P ratio (area over perimeter) for both dendritic and globular structures. By longer holding time, the interfacial area between the liquid and primary particles is reduced which is an indication of morphological evolution of primaries. This is well depicted in Fig. 7.2. The as-cast structure has a great influence on the kinetics of evolution and as shown, the evolution rate is greater for dendritic structure. The highly branched dendritic structure has a large solid–liquid interface which is equivalent to greater driving force toward area reduction, greater reaction kinetic.

As reported by other researchers [1–3], thixocast SSM structure is directly affected by the as-cast microstructure. This is to say that for a fully developed dendritic structure, the transformation to globular morphology is very unlikely and requires very long reheating period. The effect of isothermal holding time within the mushy zone on globularization is shown in B-treated samples in Fig. 7.3. In addition, there is a tendency for the primary particles to thicken through

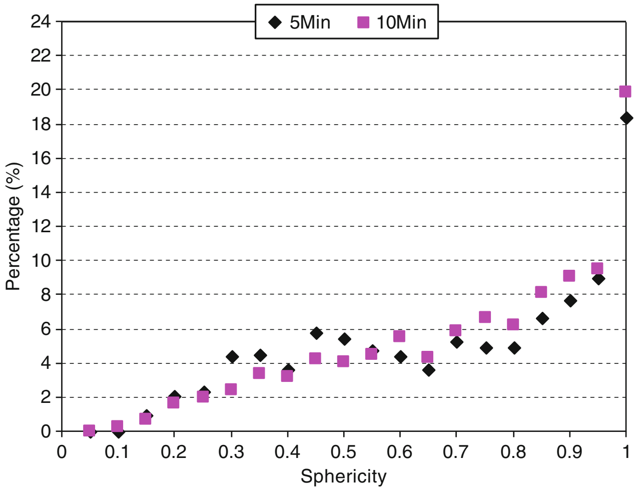

Fig. 7.3 Comparison of sphericity values for B-refined samples with different holding time (5 and 10 min)

mechanisms such as "Ostwald ripening" to reduce their interfacial area, that is, a combined process of coarsening and globularization. This is indicated by sphericity measurement (image analysis) where 10 min isothermal holding results in formation of rounder globules.

During reheating process and as a result of grain growth, parts of the liquid may be encapsulated within the coarsened grains. This entrapped liquid adversely affects the deformability of material which is associated with a reduction in the interconnected liquid phase. In fact, the percentage of the residual liquid plays an important role on the rheological behavior of the slurries. It may be regarded as a lubricant between the primary particles to ease up their movement. As for instance, by Sr addition, the surface tension of the liquid decreases and therefore easier sliding of primary particles would result in better die filling (Sect. 6.2.2).

It is also interesting to point out that the percentage of entrapped liquid decreases with increasing reheating time (Fig. 7.4). Such phenomenon may be interpreted as further segregation of aluminum onto the existing aluminum particles. The formation of entrapped liquid may be regarded as a reduction in the level of liquid within the overall 3D-interconnected liquid pool, but this cannot be with great certainty considering the difference between what is seen in 2D comparing to the real case in 3D.

7.2.2 Effect of Solidification Cooling Rate on SSM Structure

As stated in the Sect. 4.1, the entire thermal analysis cup samples solidified within the cooling rates of 1.5–2 $°Cs^{-1}$. Therefore, to study the effect of solidification cooling rate on SSM structure, new samples were solidified with much higher

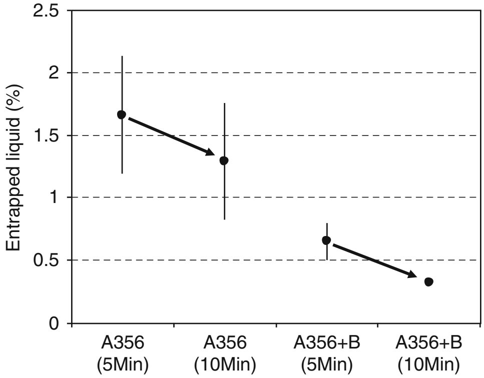

Fig. 7.4 Percentage of entrapped liquid as a function of partial remelting time

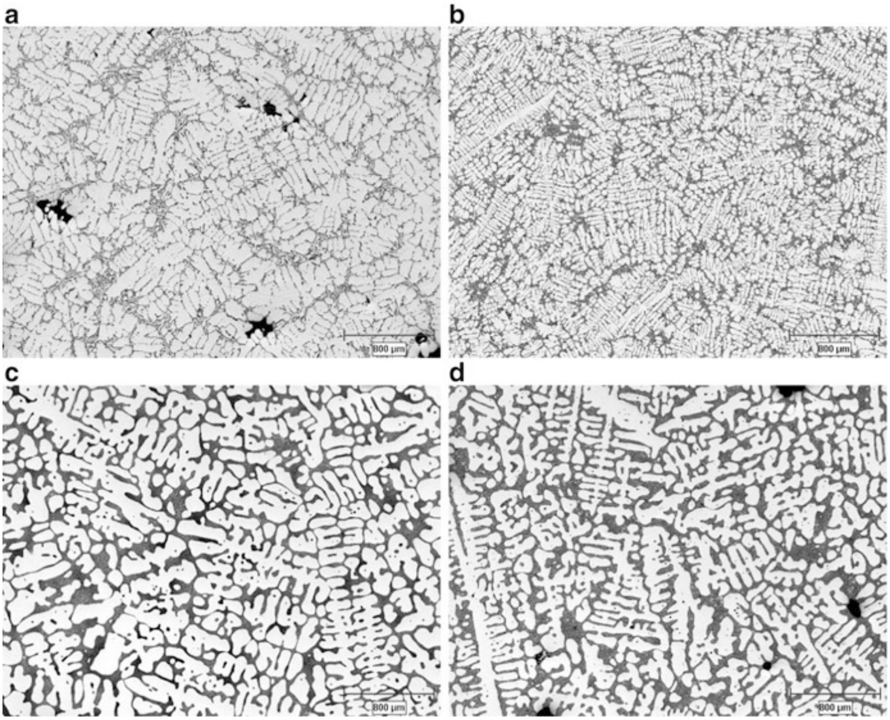

Fig. 7.5 Evolution of semi-solid structure as a function of cooling rate, A356 alloy (**a**) as-cast, ~1.5 °Cs^{-1}, (**b**) as-cast, ~11 °Cs^{-1}, (**c**) results from 10 min reheating sample "(**a**)" at 583 °C, and (**d**) results from 10 min reheating sample "(**b**)" at 583 °C

cooling rate of about 11 °Cs^{-1} with the application of compressed air. The as-cast structures are shown in Fig. 7.5a, b where higher cooling rate resulted in more compacted dendritic structure with obvious lower dendrite arm spacing "DAS" as expected. Figure 7.5c, d shows the structural evolution after 10 min holding time at

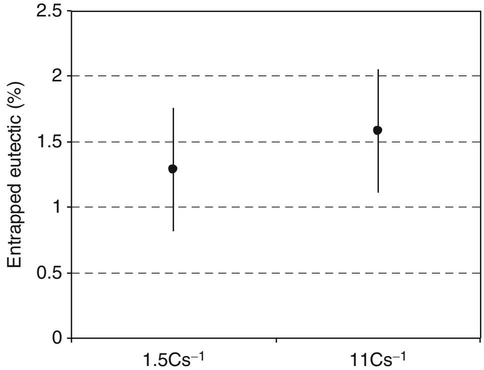

Fig. 7.6 Percentage of entrapped liquid in different cooling rates (10 min reheating at 583 °C)

about 583 °C. Both samples show dendritic structure and there is no sign of globularization. It is also difficult to ascertain if a finer as-cast billet structure has any effect on the kinetics of morphological changes as it is expected to be the case due to higher driving force initiated from larger surface area for the finer structures. Such conclusion required a full quantitative analysis which is beyond the scope of this chapter. The measured area of the entrapped liquid is shown in Fig. 7.6. Interestingly, the higher cooling rate here resulted in higher percentage of entrapped liquid. This may be attributed to finer dendritic structure having larger interfacial area which eventually results in higher number of liquid pools for faster cooled sample for this specific reheating time/temperature.

7.2.3 Addition of Various Refiners

A comparison between unrefined and refined samples is shown in Fig. 7.7. Partial remelting of B-refined alloy leads to the formation of α-Al globules with the added bonus of uniform distribution of eutectic mixture. Polarized light micrographs confirm that in the untreated and to some extent in Ti−B-treated samples, the individual particles do not essentially initiate independently from different nucleants and the concept of globule size measurement is not reasonable. Consequently, the grain size measurement was done in the entire experiments as depicted later in a graph, Fig. 7.8.

Untreated alloy has the largest grain size with nonhomogeneous size distribution considering the span of its standard deviation bar in Fig. 7.8. The unique size distribution relates to the B-refined alloy which shows the smallest standard deviation. Economically, longer reheating time has shortcomings such as higher energy consumption as well as nonuniform liquid distribution within the billet due to the gravitational force. On a microstructural stand point, increasing the duration of partial remelting leads to coarsening of primary α-Al globules as shown in Fig. 7.9 where the average circular diameter of globules was increased. However, it is believed that for this experimental condition, increasing the sphericity and

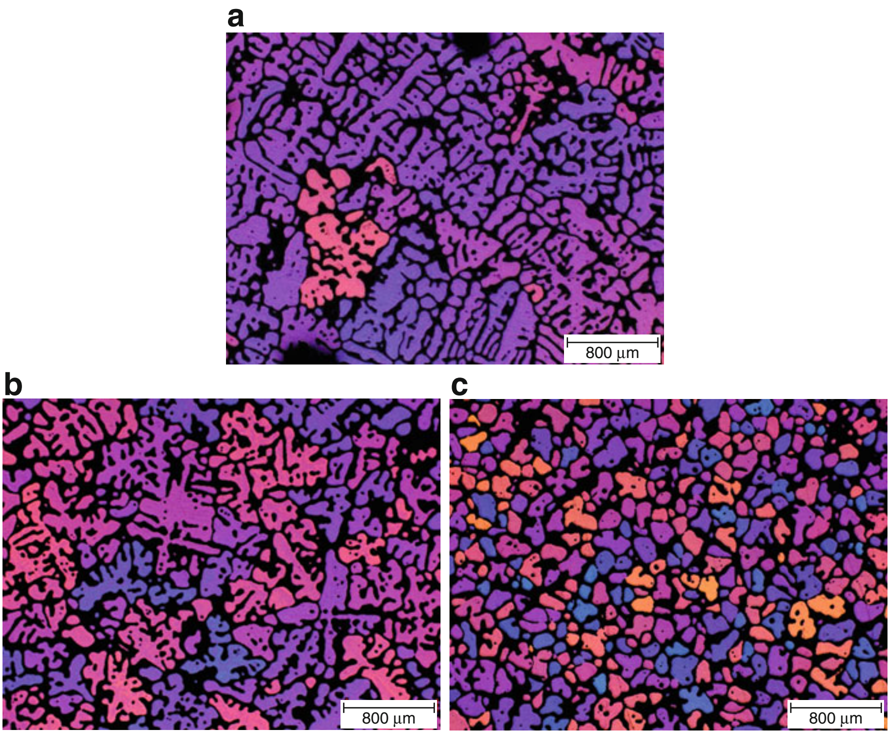

Fig. 7.7 Polarized light micrographs showing the effectiveness of refiners (10 min reheating time, 583 °C) (**a**) A356, untreated, (**b**) A356 + 622 ppm Ti + 110 ppm B, and (**c**) A356 + 226 ppm B

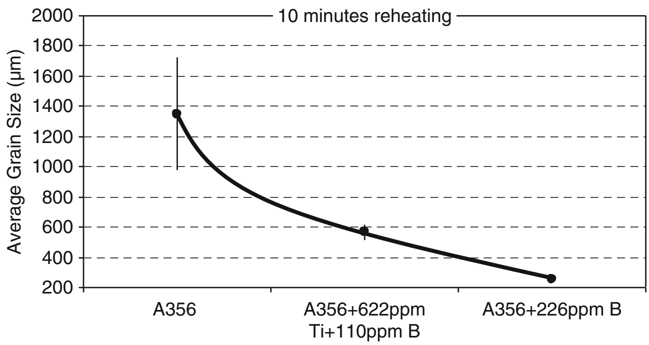

Fig. 7.8 Grain size variation according to treatment

globularity is much more important than the slight increase in the size of particles. By having more spherical primary particles, the flowability improves and consequently the viscosity decreases, Sect. 4.2.

Figure 7.10 compares the typical globule morphology of Ti/B and B-refined samples. As confirmed by quantitative metallography, the entrapped liquid content of B-refined sample is reduced by 4–5 times compared to the other samples (Fig. 7.11).

Fig. 7.9 Average circular diameter and percentage of particles having sphericity >0.8 (%)

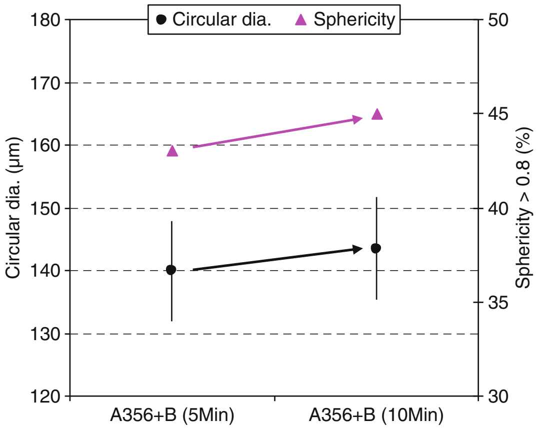

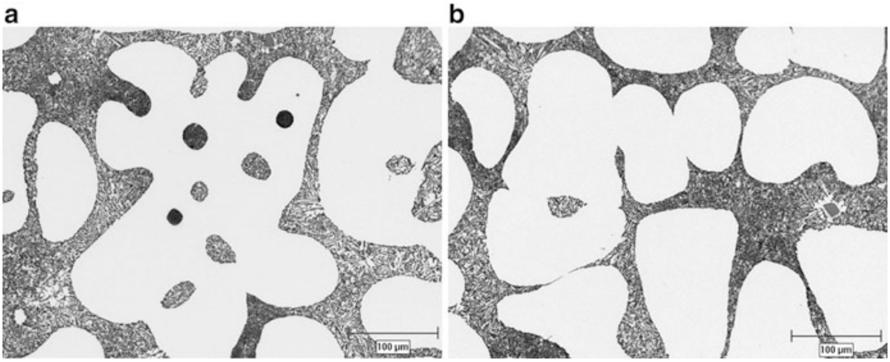

Fig. 7.10 Entrapped eutectic with different treatment (reheating time: 10 min) (**a**) A356 + 622 ppm Ti + 110 ppm B and (**b**) A356 + 226 ppm B (water quenching produces very fine Si in the eutectic)

Fig. 7.11 Percentage of the entrapped liquid (reheating time: 10 min)

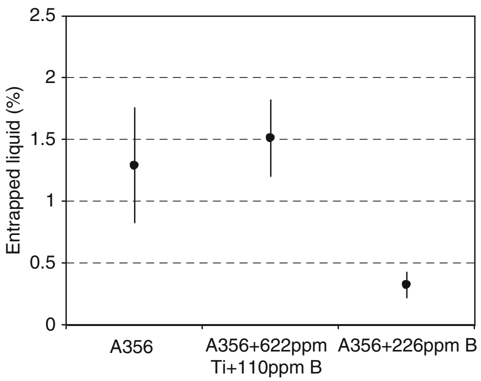

7.3 Thixocasting of EMS Billets

Binary Al–7 % Si alloys (6.7–6.9 % Si and 0.8–0.81 % Fe) were prepared and cast at two different cooling rates by pouring the molten metal in copper and sand molds at various pouring temperatures. After EMS application, samples were cooled to room temperature. For the experiments without stirring, the liquid was poured into the same molds and allowed to air cool. For thixocasting (reheating to semi-solid region), samples were cut from the transverse sections (200 mm from the bottom of EMS billets), in areas between the billet center and wall, and were reheated in an induction furnace. The reheating cycle included 2–3 min of heating up to 583 ± 3 °C and 10 min holding time at this temperature followed by water quenching (about 38–40 % fraction solid according to ThermoCalc calculations). Temperature variation during the tests was monitored by attaching thermocouples to both the billet center and the wall. More details were explained in Sects. 4.1.1.3 and 5.4.

7.3.1 Sand Mold

The polarized light micrographs in Fig. 7.12 show microstructural evolution due to variant pouring temperatures, stirring application, and reheating for thixocasting process (as-cast microstructures of these samples were presented in Chap. 5, Fig. 5.31). During isothermal holding, the eutectic is remelted while the primary α-Al phase ripened. There is also a driving force toward reduction of interfacial area between liquid and primary α-Al particles which in optimum condition leads to globularization.

Conventional samples with high pouring temperatures preserved their coarse dendritic structure even after 10 min reheating time. The very coarse structure seems to form a solid network with full 3D interconnections with a relatively high proportion of intragranular liquid. Reducing the superheat results in the evolution of the α-Al particles to rosette/equiaxed which elaborated in Sect. 5.4. By EMS application and consequent fragmentation of primary dendrites, the as-cast structure is well suited for additional morphological changes (spheroidization) through reheating process and encapsulation of the liquid phase by becoming mostly intragranular. Globule size is a bit larger within the high superheated samples but its size is reduced by lowering the superheat which is associated with the higher number of favorite nucleation sites, thermal and solute convection, and fragmentation of primary dendrites.

As described in Sect. 4.3, there is a difference between globule and grain size. Globules are primary particles which are apparently detached from each other however by applying a polarized light; it is evident that the neighbouring individual particles might have a connection from underneath of the plane of polished surface. As a result, similar color adjacent globules specify a particular grain. By this method, grains could be differentiated from globules and

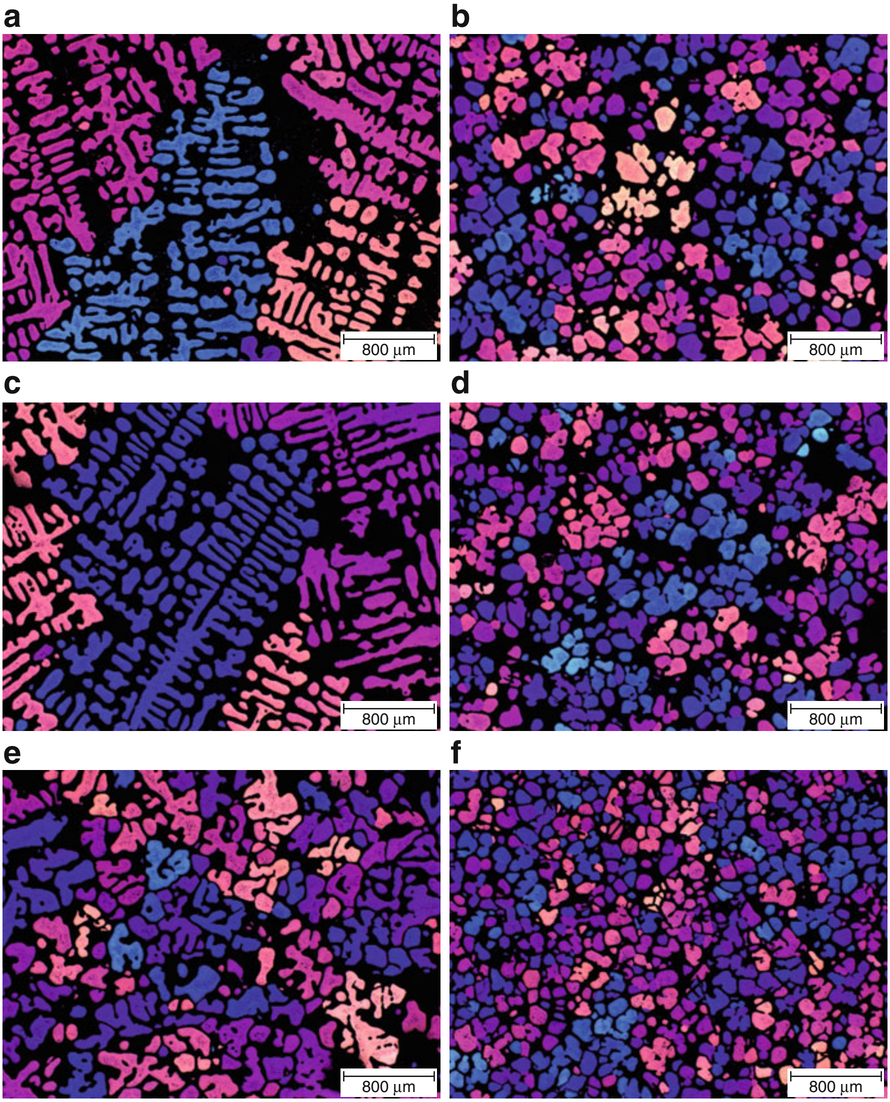

Fig. 7.12 Polarized light micrographs showing the effect of pouring temperature (690 °C "**a, b**", 660 °C "**c, d**", and 630 °C "**e, f**") and stirring on the grain and globule size variations in the sand mold casting (samples reheated at 583 °C for 10 min); (**a**), (**c**), and (**e**) conventional and (**b**), (**d**), and (**f**) EMS-stirred

Fig. 7.13 shows measured particle size of conventional and EMS reheated samples (particle size measurement by image analysis excluded all the entrapped eutectic areas). It is worth noting that the concept of globule size measurement in conventional cast samples is not completely valid which is associated with the errors related to the sectioning of dendritic branches as described in Sect. 4.3.

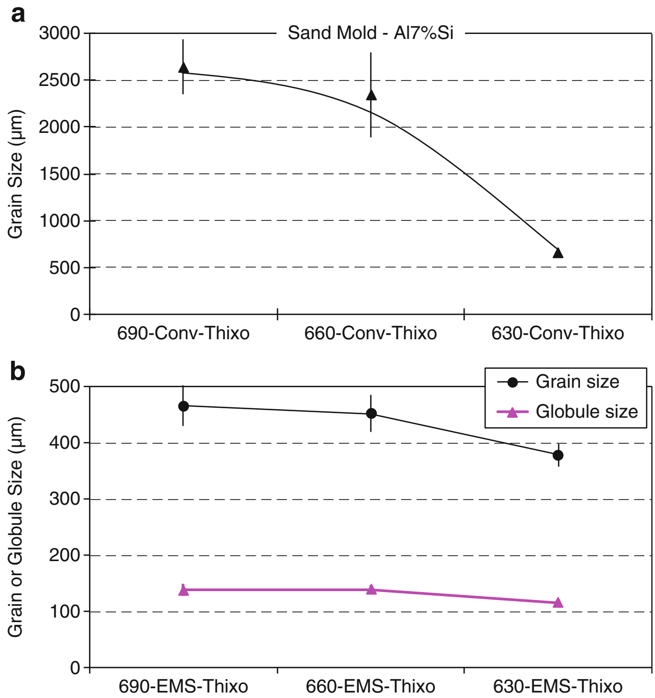

Fig. 7.13 Grain/globule size measurements in sand mold thixocast (**a**) conventional and (**b**) EMS-stirred samples (the numbers on X-axis are pouring temperatures of the billet) [4]

For conventional thixocast samples, the primary α-Al morphology is identical to the conventional cast samples (Figs. 5.31 and 7.12), although growth is noticeable due to reheating process. As a result, there is not much difference between the average grain size values (Figs. 5.34 and 7.13). In the EMS thixocast graph, Fig. 7.13b, both the grain and the globule sizes are presented. In contrast to the conventional samples, there is no sudden reduction in grain size and the values of globule size have a considerable difference from grain size values.

Agglomeration of primary particles are evident by examining the microstructure at higher magnifications, see for example Fig. 7.14. As it is clear, the particles become interconnected by solid necks and spheroidized by material transport specifically through the neck area which has a negative radius of curvature. These agglomerates are formed due to the sintering processes being activated with prolonged holding time (may be referred as coalescence ripening). Longer holding time and resultant agglomeration may encapsulate the eutectic mixture inside and form entrapped liquid area.

Selected results of image processing are presented in Fig. 7.15. By lowering the pouring temperature from 660 to 630 °C, average globule size reduced by ~15 %. Superheat reduction promotes the equiaxed particles formation with the added

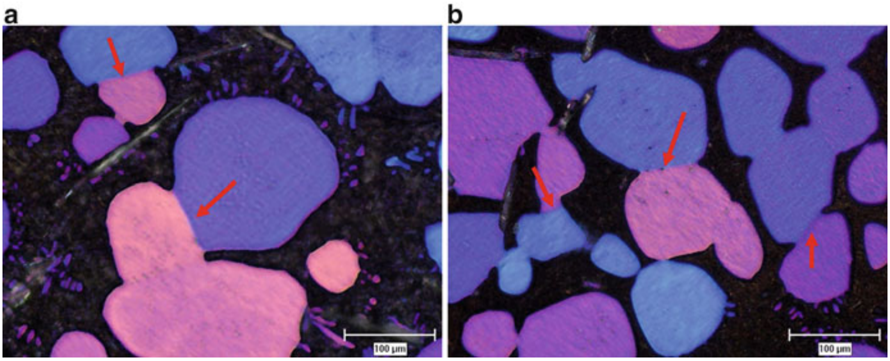

Fig. 7.14 Sintering of globules, EMS billets poured at (**a**) 690 °C and (**b**) 630 °C (sand mold, samples reheated at 583 °C for 10 min)

bonus of more nucleation sites as proven by the primary α-Al number density which is increased abruptly at 630 °C (Fig. 7.15a).

The as-cast structure is a function of pouring temperature and the greater the superheat, the structure is more dendritic. This concept is quite clear in the form of percentage of the primary α-Al particles having certain aspect ratio. By lowering the pouring temperature in conventional samples, the concentration of particles with an aspect ratio >2 decreases (Fig. 7.15b). The lowest amounts of primary particles with aspect ratio >2 were observed in EMS billets with a reasonable difference to that of the reheated conventionally cast samples.

By decreasing the pouring temperature, particles become more spherical and as a result, percentage of particles having sphericity values greater than 0.8 increases. Comparing the conventional and EMS-treated samples, it is clear that the percentage of particles having sphericity >0.8 is higher for EM stirred samples. In rheological studies, more spherical particles results in lower viscosity (Sect. 4.2) which is expected to induce better flowability and filling of the die cavity during high pressure diecasting.

Entrapped liquid has an impact on the viscosity of the semi-solid slurries and less entrapped liquid results in better fluidity [5–7]. Conventionally cast samples have a tendency to entrap the liquid which is normal in dendritic structure. Casting the billets with high superheat leads to a complex and massive dendritic structure which could encapsulate a portion of the liquid formed during reheating. Accordingly by superheat reduction, the structure tends to form rosette/equiaxed primary α-Al particles with less probability of liquid entrapment. In the case of EMS samples, the structure not only transforms to globules but also contains the least entrapped liquid, Fig. 7.16.

It is observed that the majority of entrapped liquid in the EMS samples initiates from liquid encapsulation by the surrounding globules, while for conventional samples, the main source is the liquid between secondary or tertiary dendrite arms. This notion is depicted in Fig. 7.17 for billets poured at 690 °C. This may have some effect on the homogeneity of entrapped liquid where a more uniform

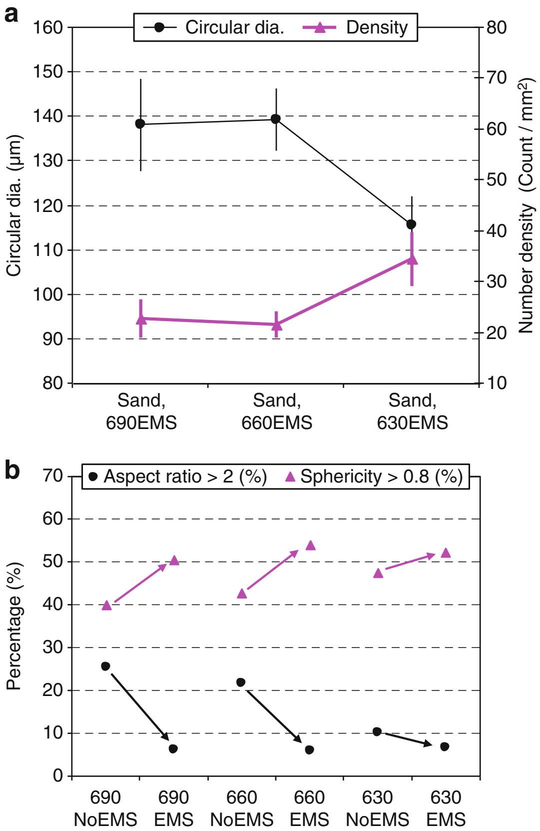

Fig. 7.15 Image analysis results from various pouring temperatures/application of EMS, sand mold thixocast [4]

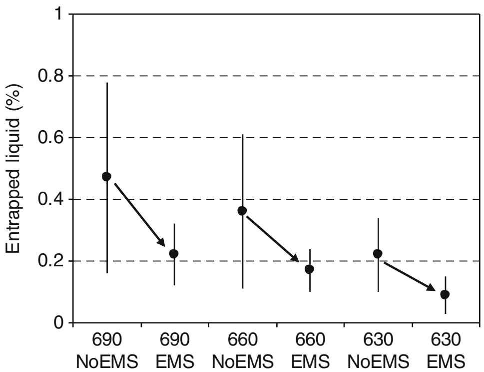

Fig. 7.16 Entrapped liquid measurement, sand thixocast [4]

composition is expected for the entrapped liquid for EMS thixocast billets. Conventionally cast thixo billets have entrapped liquid that is more characteristics of the interdendritic segregation.

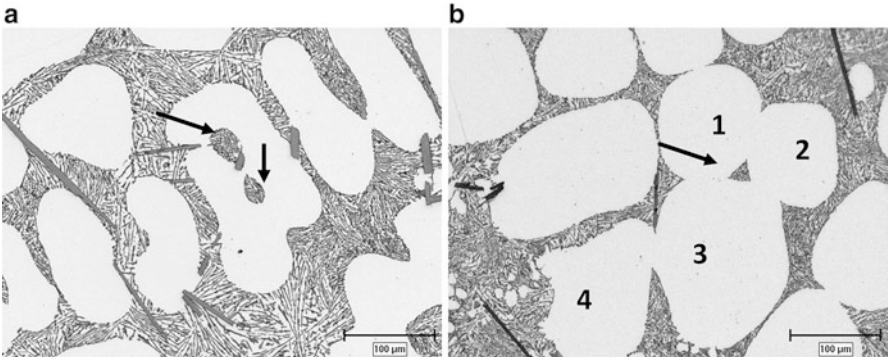

Fig. 7.17 Entrapped liquid in billets poured at 690 °C (**a**) conventional and (**b**) EMS (numbers show the globules and arrows show the liquid pockets)

7.3.2 Copper Mold

Figure 7.18 shows the microstructural evolution of copper mold cast samples by reheating at ~583 °C. Conventional thixo structures have dendritic morphology characterized by continuous solid network and liquid pockets. In contrast to the sand mold cast billets, casting in copper mold leads to thinner dendrite branches and smaller dendrite arm spacing (DAS). Lowering the pouring temperature results in rounder and more isolated particles with least entrapped liquid (Fig. 7.18a, c, e). EMS-reheated structures, however consist of almost all globules with an average size of about 100 µm even at higher superheats. The globules are well distributed within the eutectic network and nearly all the eutectic liquid pools are intergranular (Fig. 7.18b, d, f).

The trend of grain size values for the reheated conventional samples is similar to that of the as-cast structure (Fig. 5.40) including the direct relation to the pouring temperature (Fig. 7.19a). Comparing the grain/globule size values for sand and copper mold billets shows that by stirring, the grain/globule size values are getting closer, indicating almost independent relationship to the casting condition. In other words, the application of EMS diminishes the importance of the cooling rate and pouring temperature which could control the globule and grain size during reheating.

As mentioned in Sect. 4.3.1, sintering and coalescence of particles are parts of isothermal holding. Figure 7.20 shows typical sintering incidents in copper cast samples.

The process of globularization and refinement of the primary α-Al particles are shown in Fig. 7.21. In EMS samples, the average globule size reduces by lowering the pouring temperature. Interestingly, the rate of globule size reduction is lower than the sand mold cast specimen while the increasing rate of number density is higher indicating the importance of the as-cast structure.

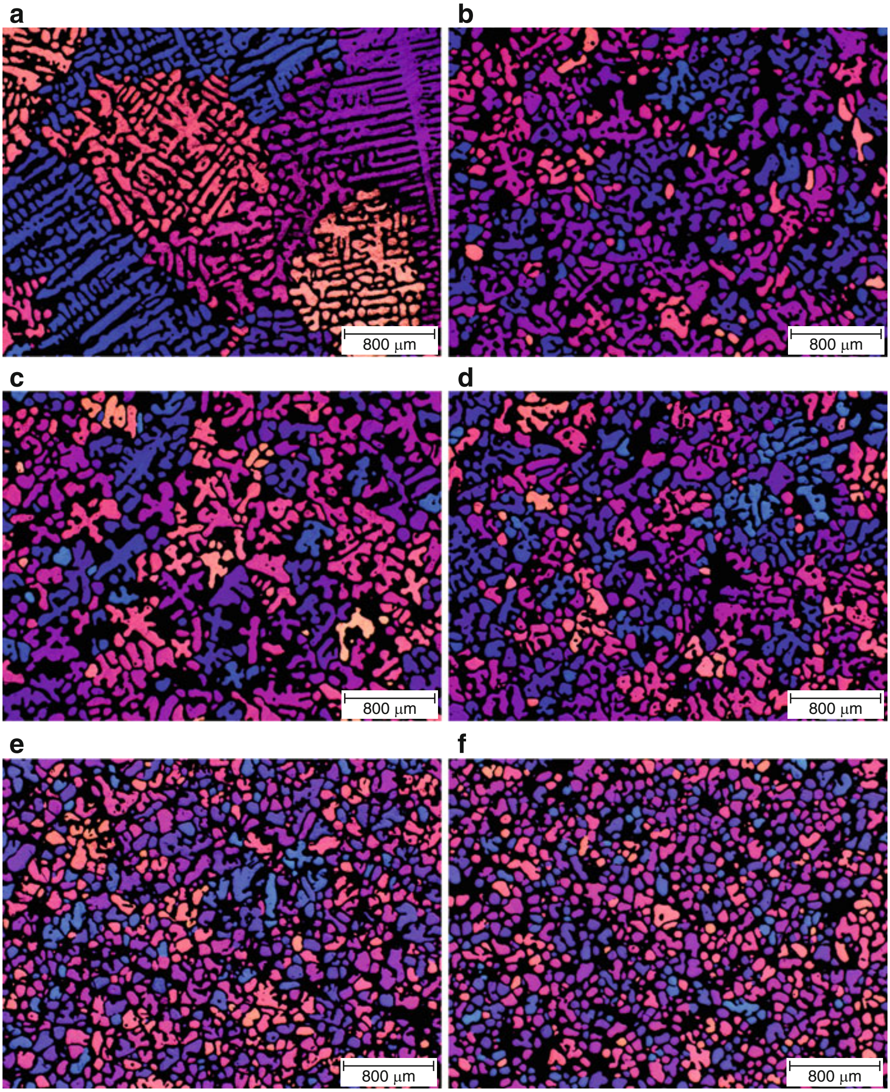

Fig. 7.18 Polarized light micrographs showing the effect of pouring temperature (690 °C "**a, b**", 660 °C "**c, d**", and 630 °C "**e, f**") and stirring on the grain and globule size variations in the copper mold casting (samples reheated at 583 °C for 10 min) (**a**), (**c**), and (**e**) conventional and (**b**), (**d**), and (**f**) EMS-stirred

The aspect ratio exhibits the same trend as sand cast samples, and the percentage of particles with aspect ratio >2 decreases with decreasing pouring temperature in both conventional and EMS samples; however, the reduction rate is higher for conventional samples. In fact, during the reheating process, an initial higher cooling rate (copper mold) results in the billets having greater potential for microstructural

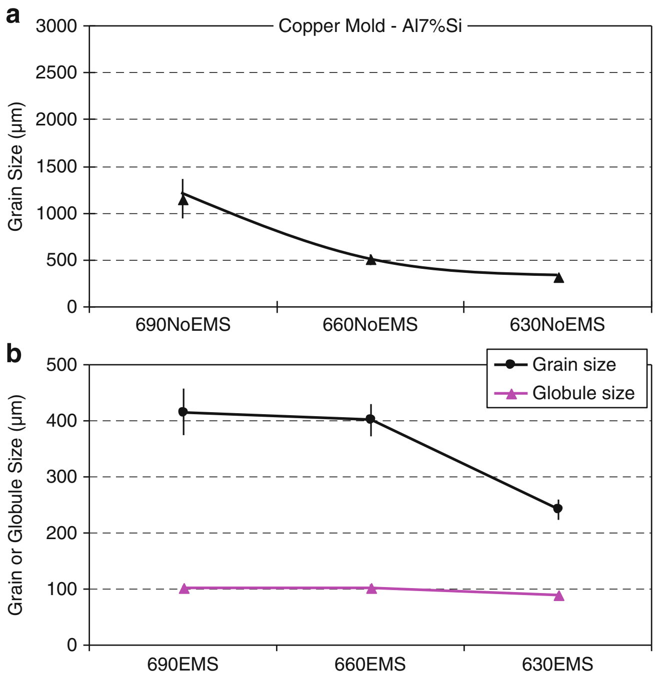

Fig. 7.19 Grain/globule size measurements in copper mold thixocast (**a**) conventional and (**b**) EMS-stirred samples (the numbers on X-axis are pouring temperatures of the billet) [4]

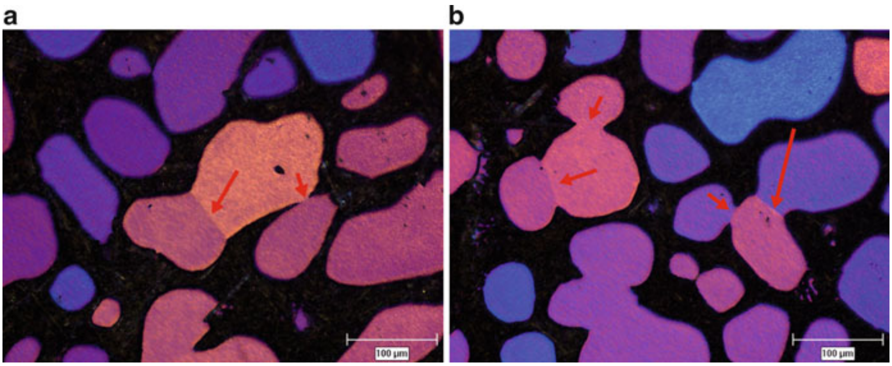

Fig. 7.20 Sintering of globules, EMS billets poured at (**a**) 690 °C and (**b**) 630 °C (copper mold, samples reheated at 583 °C for 10 min)

evolution, that is, larger interfacial area, and this is evident by comparing the results, Figs. 7.15 and 7.21. By lowering the superheat, the percentage of particles with sphericity value greater than 0.8 increases and the maximum value belong to EMS and lower superheated samples. In addition, the sphericity values are greater in comparison to the sand mold cast samples.

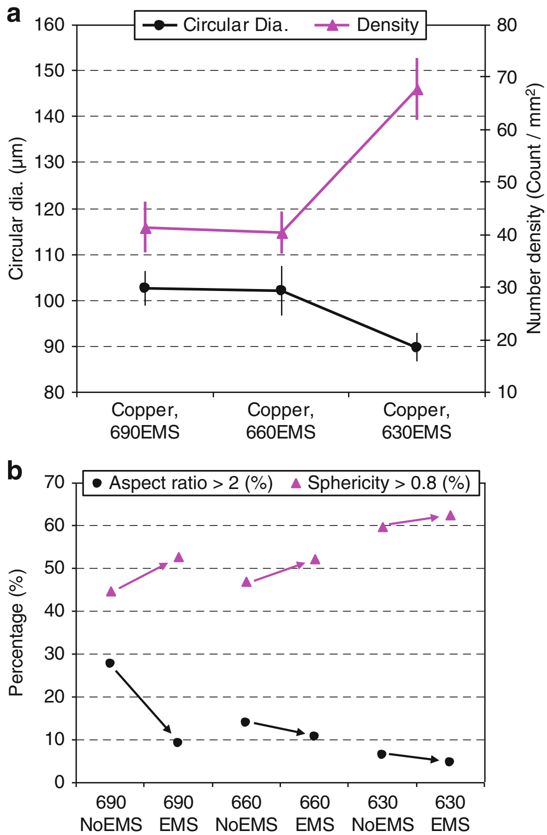

Fig. 7.21 Image analysis results from various pouring temperatures/application of EMS, copper mold thixocast [4]

According to Loué and Suéry [1], during partial remelting, coarsening first proceeds predominantly through coalescence of dendrite arms. As the dendrite arms of the same grain have a perfectly matching crystallographic orientation, this results in high quantity of intragranular liquid which depends on the cooling rate. In the case of EMS samples, the coalescence of short dendrite arms leads to almost globular structure with a smaller amount of liquid pocket. The formation of spherical particles could be assisted by lowering the pouring temperature and thus having higher probability of equiaxed grains formation. Figure 7.22 illustrates the concept within the copper cast structures with high superheat value.

Comparing the micrographs with those of sand mold structures suggests that the percentage of liquid encapsulation in the conventional castings is also dependent on the cooling rate and it is higher for lower cooling rate. Quantitative results also reveal that cooling rate has a key role to play on the liquid encapsulation and its percentage is higher for lower cooling rates. In general, higher cooling rate during solidification leads to more uniform (less standard deviation) liquid entrapment throughout the sample. It is worth noting that the efficiency of EMS in refining the structure becomes more noticable at lower cooling rate during solidification (Figs. 7.16 and 7.23).

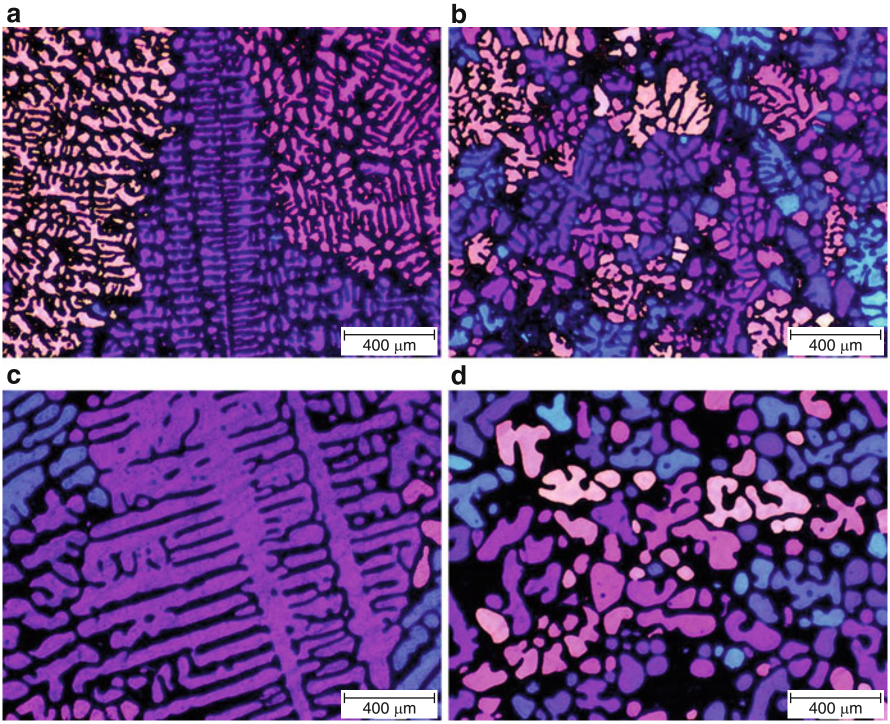

Fig. 7.22 Copper mold samples, poured @690 °C (**a**) as-cast, conventional, (**b**) as-cast, EM stirred, (**c**) thixocast, sample "(**a**)", and (**d**) thixocast, sample "(**b**)" [4]

Fig. 7.23 Entrapped liquid measurement, copper thixocast [4]

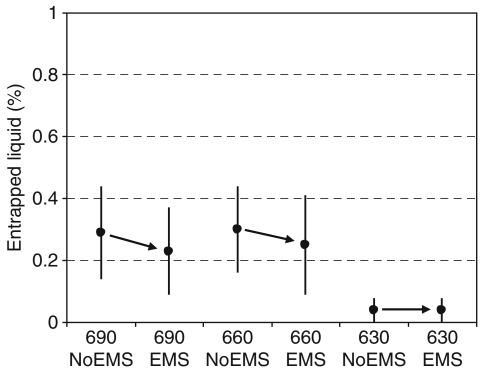

Solidification time has an impact on partial remelting procedure. Basically, the driving force for the microstructural evolution within the mushy zone is the reduction of the interfacial area between liquid and solid. This could be estimated by the area to perimeter ratio. In fact, as mentioned in Sect. 4.3, this factor has an inverse relationship with the specific surface area per unit volume of the particles,

S_v. In dendritic solidification, higher values of *P* (total solid–liquid interface length) resemble a structure with more dendrite branches. Solid–liquid interfacial length mainly depends on the solidification of the alloy. For instance, the higher cooling rate of copper mold samples leads to lower dendrite arm spacing and finer secondary and tertiary branches and therefore the interface boundary of the eutectic-primary particles increases.

The effectiveness of A/P ratio in expressing the morphological changes in the as-cast structure during thixocasting (reheating at 583 °C for 10 min) for different cooling rates and application of EMS is given in Fig. 7.24. In conventional casting method, copper cast samples have a shorter solidification time which leads to a finer and more highly branched dendritic structure and therefore the A/P is smaller. In the same condition, lowering the superheat results in an equiaxed structure which during isothermal holding transforms to a globule/rosette structure. Similarly, higher cooling rate results in finer particles with smaller value of A/P (Fig. 7.24a).

Electromagnetic stirred billets exhibited a similar trend. The higher cooling rate of the copper mold leads to smaller dendrite size, and when coupled with stirring, results in greater percentage of fragmented dendrites with better distribution within the bulk liquid. A shorter solidification time also results in a limited growth with the eventual structure containing globules with smaller size compared to those of the sand mold billets (Fig. 7.24b). It is worth noting that the correlation between A/P

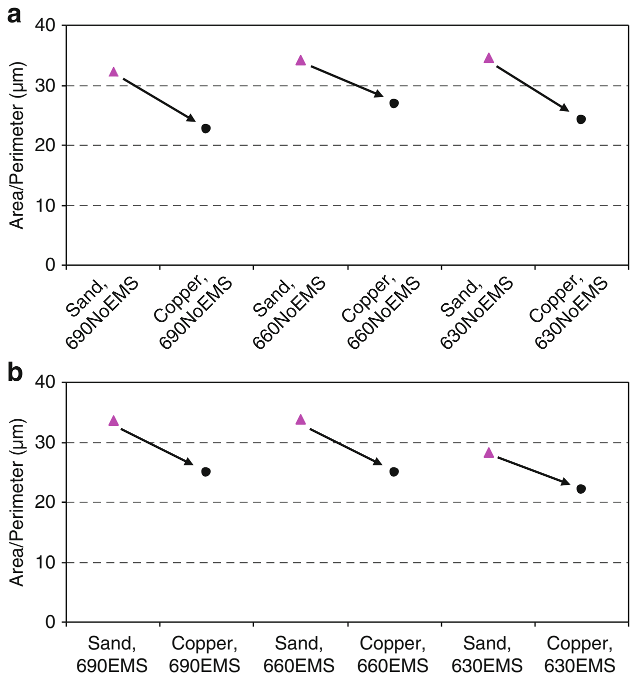

Fig. 7.24 Evolution of A/P ratio as a function of pouring temperature and stirring (*triangles* and *circles* for sand and copper molds cast samples, respectively) [4]

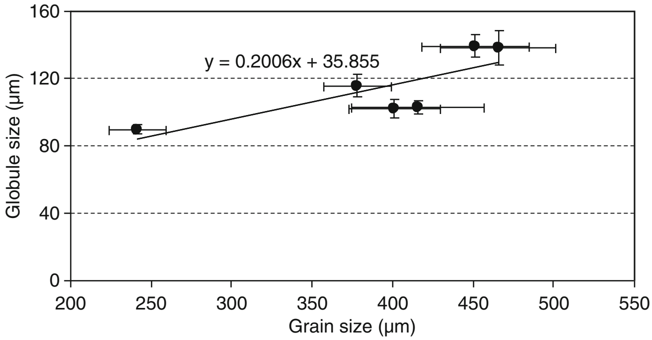

Fig. 7.25 Correlation between grain and globule size in EMS samples [4]

and application of EMS is not significant for either sand or copper molds at higher casting temperatures, 660 and 690 °C, but when temperature drops the effect of EMS on A/P ratio becomes more pronounced which is an indication of smaller particle size.

There is a direct correlation between grain/globule sizes and macro/microstructural evolution. The trend is shown in Fig. 7.25 where the smaller the grain size, the smaller is the globule size. This concept becomes complicated if one fails to differentiate between the globule and grain distinction as mentioned in Sect. 4.3.

7.3.3 Grain Refining/EMS: the Premium Choice

In Sect. 5.4, it was confirmed that electromagnetic stirring leads to fragmentation of primary phase and consequently homogeneous distribution of broken α-Al particles within the billets. A question may be raised on the influence of the refiner and vigorous agitation by EMS and whether it is favorable or not. In order to examine the benefit of grain refinement during EMS process, boron was selected as the refining agent and two series of tests were performed within the sand mold, with and without EMS application as explained in Sect. 4.1.1.3. Different pouring temperatures of 660 and 630 °C were examined and for refining objective, about 220 ppm boron was added using Al-5 % B master alloy with the final composition of Al (balance), 6.87 % Si, 0.84 % Fe, and 0.022 % B.

Figures 7.26 and 7.27 compare the resulting morphological evolution due to the boron addition/EM stirring. The primary α-Al phase has a fully columnar (dendritic) structure in the untreated sample and transforms to equiaxed morphology with the boron addition. This is evident in samples cast at higher superheat, for example, comparing Fig. 7.26a, b. However, when pouring temperature is decreased, the structure transforms to equiaxed, but finer and more spherical particles are achieved by refining process (comparing Fig. 7.27a, b). By stirring, the refining process is improved as revealed in the polarized light micrographs of

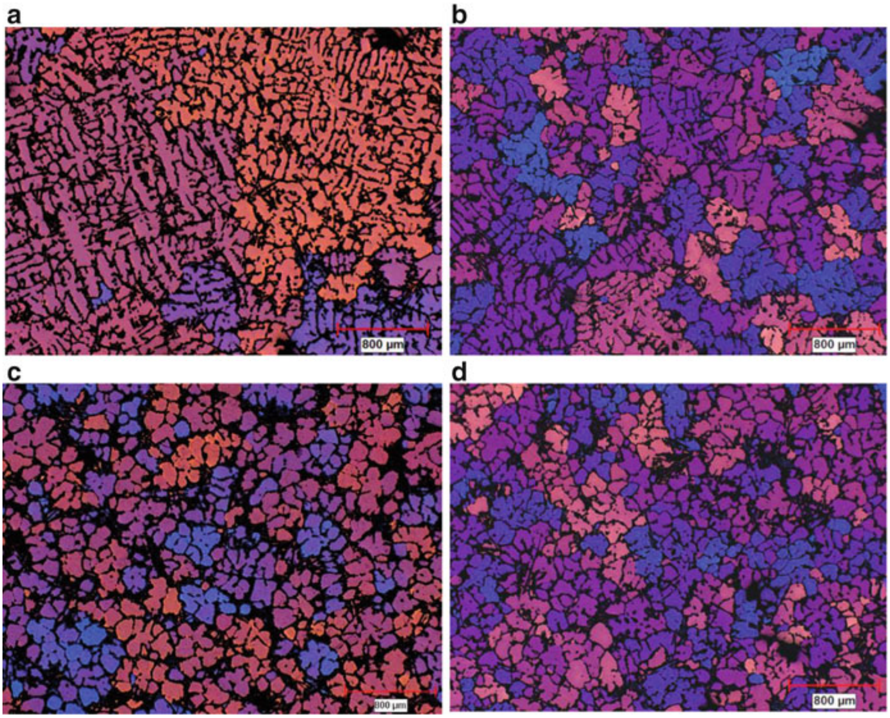

Fig. 7.26 Effects of boron addition/stirring on the formation of primary particles (sand cast, poured at 660 °C) (**a**) unstirred, unrefined, (**b**) unstirred, refined with ~220 ppm B, (**c**) EM stirred, unrefined, and (**d**) EM stirred, refined with ~220 ppm B

Figs. 7.26d and 7.27d for both pouring temperatures. The EM stirred samples show smaller and more compacted (denser) primaries.

As the pouring temperature decreases, the rate of heat extraction from the mold walls reduces and therefore a shallow temperature gradient within the bulk liquid is established (Sect. 5.2). Such temperature gradient encourages the formation of smaller primary particles with better distribution and thus more equiaxed particles will form. This concept is clearly shown by grain size measurement in Fig. 7.28a. By decreasing the pouring temperature from 660 to 630 °C, average grain size is reduced by a factor greater than 3. On the other hand by boron refining, nucleation sites increases drastically, so-called copious nucleation mechanism, and therefore smaller and more equiaxed particles were formed. It is worth mentioning that the refining impact is more pronounced in the case of higher superheats while by lowering the superheat, the shallow temperature gradient has a main contribution and as a result, the reduction in size consists of two elements which one overshadows the effect of the other (comparing ~72 % to ~56 % reduction in size for 660 °C and 630 °C, respectively).

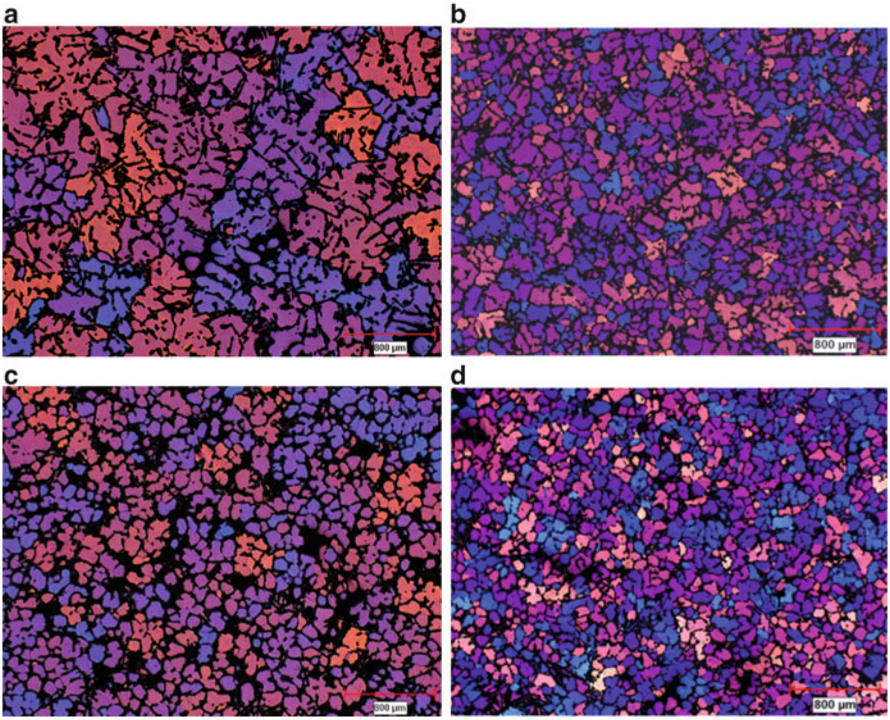

Fig. 7.27 Effects of boron addition/stirring on the formation of primary particles (sand cast, poured at 630 °C) (**a**) unstirred, unrefined, (**b**) unstirred, refined with ~220 ppm B, (**c**) EM stirred, unrefined, and (**d**) EM stirred, refined with ~220 ppm B

As described in Sect. 5.4, vigorous agitation leads to fragmentation of primary particles and the final structure is fully equiaxed. Grain size measurement (Fig. 7.28b) confirms that in the case of stirring, refiner addition is less prominent in comparison with the conventional casting, that is, stirring overshadows grain refinement.

7.3.3.1 Thixocasting of the Refined EMS Billets

Effects of isothermal holding on the aforementioned samples (Sect. 7.3.3) are shown in Figs. 7.29 and 7.30. The following points are noticeable:

- Generally, the lower the pouring temperature, the better is the results of thixocasting process. Better distribution (isolated particles) and equiaxed morphology before isothermal holding are the controlling parameters for rounder and smaller particles. This is clear through comparison of Figs. 7.29 and 7.30.
- Refining process results in the formation of more uniform equiaxed particles having less energy barrier for conversion to spherical particles through isothermal holding. During thixocasting, particles tend to reduce their energy level by

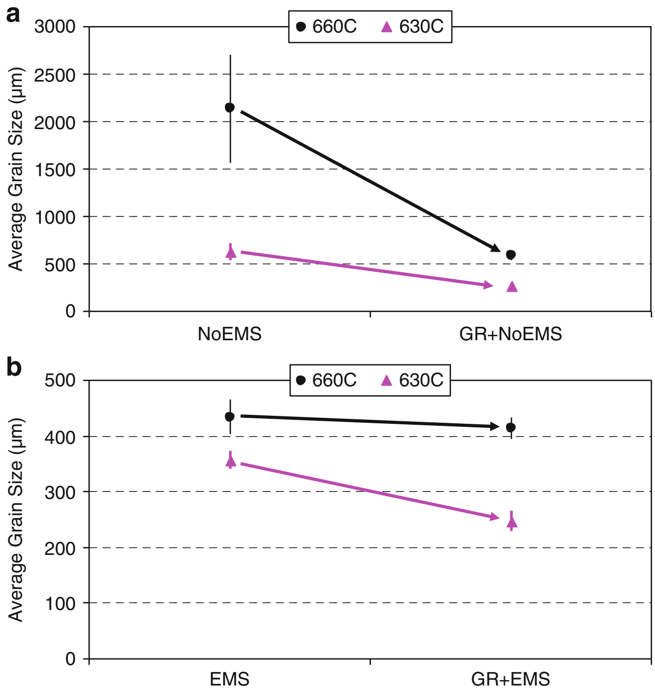

Fig. 7.28 Correlation between grain size variation and process parameters (grain refiner/stirring) (**a**) without stirring and (**b**) EM stirred

decreasing their surface area through transformation to most appropriate form (morphology) which is sphere (globule).

- Addition of refiner results in more potent sites for nucleation process rendering a larger number of particles per unit volume (number density of primary particles increases). This is apparent both in unstirred and stirred samples and it is more discernible at the lower superheats.

Figure 7.31 demonstrates the grain size evolution during the entire thixocasting experiments. Results are in line with conventional cast and/or stirred samples. Lower superheat and vigorous agitation lead to smaller and more isolated particles which are then transform to globules during isothermal holding (coarsening of primary particles is evident which is typical during isothermal holding).

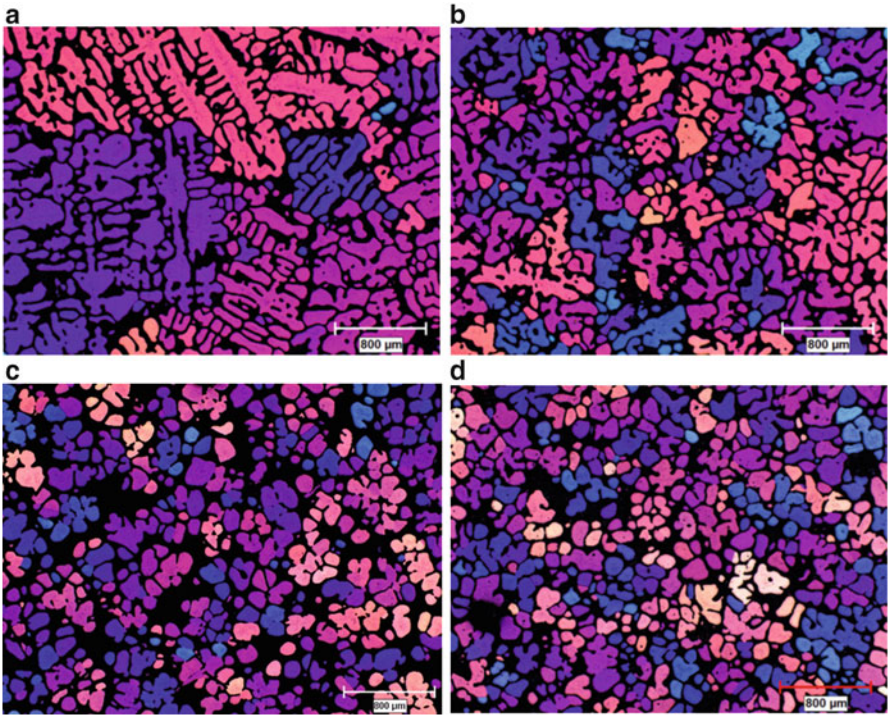

Fig. 7.29 Effects of boron addition/stirring on the formation of primary particles (sand mold cast, poured at 660 °C, reheated at 583 °C for 10 min) (**a**) unstirred, unrefined, (**b**) unstirred refined with ~220 ppm B, (**c**) EM stirred, unrefined, and (**d**) EM stirred, refined with ~220 ppm B

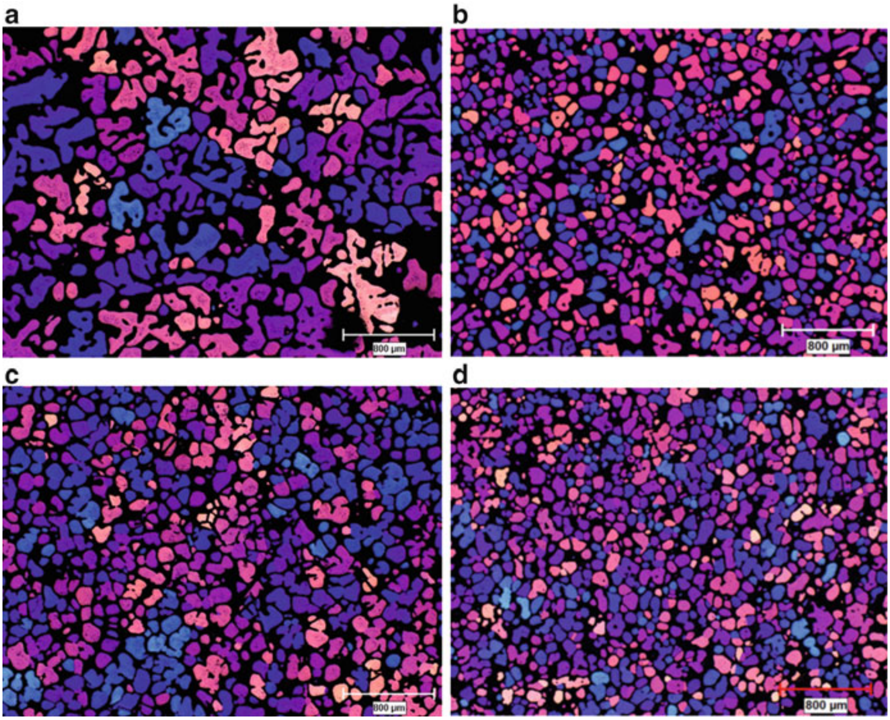

Fig. 7.30 Effects of boron addition/stirring on the formation of primary particles (sand mold cast, poured at 630 °C, reheated at 583 °C for 10 min) (**a**) unstirred, unrefined, (**b**) unstirred refined with ~220 ppm B, (**c**) EM stirred, unrefined, and (**d**) EM stirred, refined with ~220 ppm B

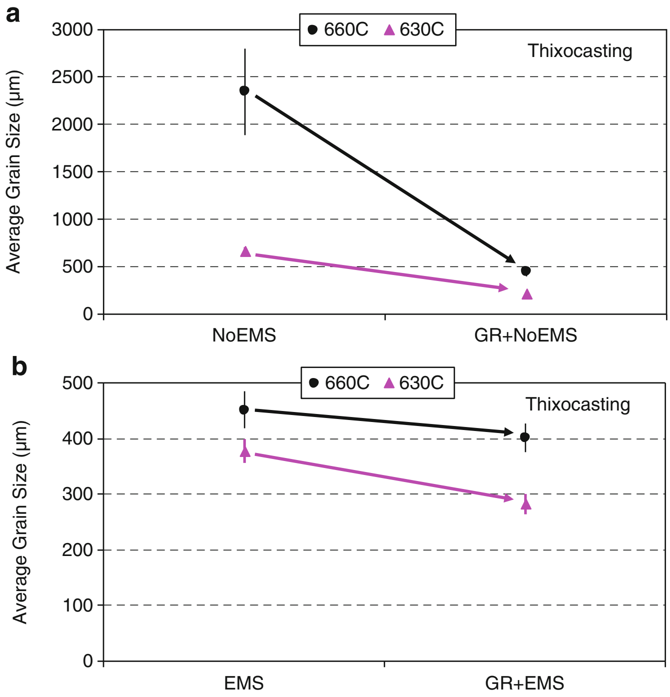

Fig. 7.31 Correlation between grain size variation and process parameters in thixocasting process (sand mold cast, reheated at 583 °C for 10 min) (**a**) without stirring and (**b**) EM stirred

References

1. W.R. Loue, M. Suery, Microstructural evolution during partial remelting of Al-Si7Mg alloys. Mater. Sci. Eng. A **A203**, 1–13 (1995)
2. Q.Y. Pan, M. Arsenault, D. Apelian, M.M. Makhlouf, SSM processing of AlB2 grain refined Al-Si alloys. AFS Trans. **112**, (2004), Paper 04-053
3. H. Wang, C.J. Davidson, D.H. St John, Semisolid microstructural evolution of AlSi7Mg alloy during partial remelting. Mater. Sci. Eng. **A368**, 159–167 (2004)
4. S. Nafisi, R. Ghomashchi, Microstructural evolution of electromagnetically stirred feedstock SSM billets during reheating process. J. Metallogr. Microstruct. Anal. **2**(2), 96–106 (2013)
5. D.H. Kirkwood, Semi-solid metal processing. Int. Mater. Rev. **39**(5), 173–189 (1994)
6. Z. Fan, Semisolid metal processing. Int. Mater. Rev. **47**(2), 49–85 (2002)
7. M.C. Flemings, Behavior of metal alloys in the semi-solid state. Metal. Trans. A **22A**, 952–981 (1991)